4.1 USING SPATIAL AVERAGING FOR COMPUTING EDDY FLUXES

Matthias Mauder[1,*], Raymond L. Desjardins[1], Ian MacPherson[2], Elizabeth Pattey[1], Zhiling Gao[1], Ronald van Haarlem[1]

[1] Agriculture and Agri-Food Canada, Research Branch, Ottawa, Canada

[2] National Research Council, Institute for Aerospace Research, Flight Research Laboratory, Ottawa, Canada

1. INTRODUCTION

During the late 1980s, it became obvious that the energy balance at the earth's surface could not be closed with experimental data (Desjardins, 1985; Chahuneau et al., 1989). The available energy, i.e. the sum of the net radiation ($-Q_s^*$) and the ground heat flux (Q_G)

$$-Q_s^* - Q_G = Q_H + Q_E \,, \qquad (1)$$

was found in most cases to be larger than the sum of the turbulent fluxes of sensible (Q_H) and latent (Q_E) heat. For example, Aubinet et al. (2000) conclude that the energy balance tends to be more or less unclosed, an indication that non-vertical or non-turbulent fluxes need to be incorporated in the budget calculation, or that there are substantial errors in other energy flux terms which lead to an underestimation of available energy fluxes. In a review of 11 published articles, the sum of convective energy fluxes was found to be 89% of available energy (Sakai et al., 2001). A general lack of energy balance closure was also found in another study about 20 FLUXNET sites (Wilson et al., 2002). The mean imbalance was in the order of 20%.

Eddy covariance measurements are widely used to study the atmosphere-biosphere exchange. However, there are some issues that must be resolved. One of them is that complete energy balance closure is usually not achieved even during the daytime when measurement conditions are usually favorable. We believe that transport in eddies that cannot be captured by common averaging times of 30 min to 60 min can explain a major part of this systematic underestimation. We propose applying spatial averaging over long enough distances in order to minimize this underestimation. An advantage of spatial averaging is that it can resolve quasi-stationary circulations, which is almost impossible for flux computations based on temporal averaging.

* *Corresponding author address:* Matthias Mauder, Agriculture and Agri-Food Canada, 960 Carling Ave., Ottawa, Ontario, Canada, K1A0C6; email: mauderm@agr,gc.ca

2. MESOSCALE FLUX CONTRIBUTIONS FROM 1-DIMENSIONAL AIRCRAFT MEASUREMENTS

The data for this study were measured on board of the Twin Otter research aircraft (MacPherson et al., 2001) of the Canadian National Research Council (NRC) along a 115 km transect in May of 1994 as part of the BOREAS (Boreal Ecosystem - Atmosphere Study). The Twin Otter was equipped to measure fluctuations of wind, temperature, water vapor, CO_2 and O_3 at a frequency of 16 Hz (MacPherson, 1996). The measurement height was approximately 30 m at a groundspeed of 60 m s^{-1}. The 'Candle Lake Run' stretched from 53.57ºN, 106.40ºW to 53.98ºN, 104.29ºW in central Saskatchewan, Canada (Figure 1).

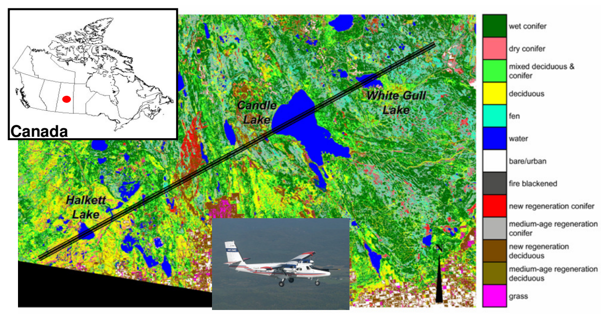

Figure 1: Land cover classification of a Landsat Thematic Mapper (TM) image of the area around Candle Lake from 2 September 1994 (after Hall et al., 1997). The flight track of the NRC Twin Otter Candle Lake Run is indicated by a triple line.

Wavelet transform was employed to analyze these data since this method does not require stationarity nor homogeneity, in contrast to Fourier analysis. It gives quantitative information, where in space and on what wavelength flux contributions occur. It allows distinguishing between small-scale turbulence (< 2 km) and mesoscale fluxes (> 2 km). Source code provided by C. Torrence and G. Compo (available at: http://paos.colorado.edu/research/wavelets/) was modified to conduct the wavelet analysis of the Twin Otter aircraft data. The methodology applied is based on the study of Mauder et al. (2007). The wavelet covariance between the vertical wind velocity w and a scalar s is equivalent to its flux density F.

$$F = \frac{\delta p \delta t}{N C_\delta} \sum_{n=0}^{N-1} \sum_{p=0}^{P} \frac{W_w(n,p) W_s^*(n,p)}{a(p)}. \qquad (2)$$

This value can be calculated by summation of the cross-scalogram matrix over the entire flight track, containing *N* elements, and over the scale range that was not affected by the cone of influence COI, containing *P* elements. A value of 0.25 was chosen for δp, a nondimensional factor that determines the spacing between discrete scales of the wavelet transform, δt is the time step of the time series (0.03125 s), and $a(p)$ is the scale parameter of the wavelet transform. The factor C_δ, that is required for the reconstruction the band pass filtered original time series from the wavelet transform, is a constant for each wavelet function and has a value of 0.776 for the Morlet mother wavelet (Torrence and Compo, 1998).

Figure 2 shows the cross-scalograms for the flight between 1041 and 1116 CST (Central Standard Time) on 25 May 1994. The Twin Otter was heading west-south-west (245º) during this flight. The wind direction was 172º. The segmentation of the flight track into nine land cover types as shown in Figure 2 is in accordance with MacPherson (1996).

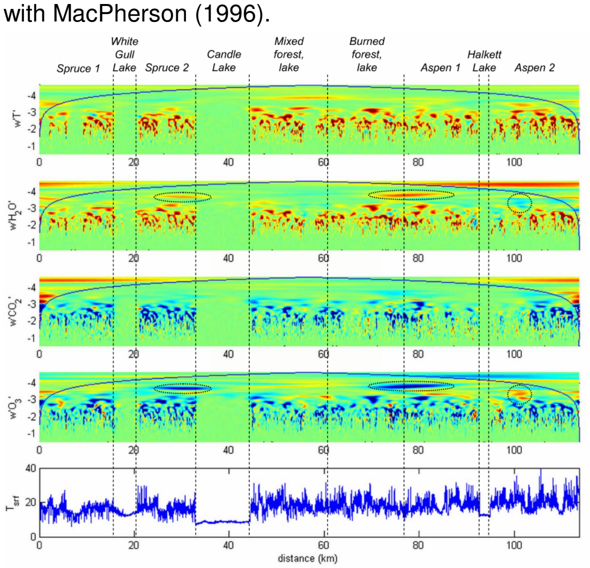

Figure 2: Wavelet cross-scalograms between w and T, H_2O, CO_2, and O_3. The common logarithm of the wavenumber (m^{-1}) is given on the ordinate of the cross-scalograms. Red colors indicate positive flux contributions, blue denotes negative flux contributions, and green tones stand for areas of fluxes close to zero. Land cover types are given on the top. Similar mesoscale structures in w′H2O′ and w′O3′ are indicated by dotted ellipses. The cone of influence (COI) is indicated by a blue line. Surface temperature (ºC) is shown in the bottom subplot for orientation. Flight BOREAS, 1041 – 1116 CST, 25 May 1994 (Mauder et al., 2007).

The intensity of the colors in Figure 2 is proportional to the flux contribution. No obvious differences could be found between the fluxes over different terrestrial land cover types. In contrast, the three major lakes were well-represented in the cross-scalograms. All scalar fluxes were close to zero over the lakes for the small-scale turbulent part (< 2 km) due to stable stratification. Some mesoscale structures reached over the eastern shore of Candle Lake, though. The mesoscale structures of water vapor and ozone fluxes appeared to be relatively similar (see dotted ellipses in Figure 2). No equivalent structures occurred for the sensible heat flux and the CO_2 flux.

The measured fluxes were partitioned into small-scale turbulence and mesoscale structures through integrating the wavelet cross-scalogram for wavelengths smaller than 2 km and longer than 2 km separately. The flux contributions of these scale classes are shown in Figure 3 for the entire run. The mesoscale transport was on the order of 10% of the turbulent flux for all four scalar quantities investigated. The same wavelet analysis was conducted for twenty flights at the same location. These represent different times of the day and different days of the year (Mauder et al., 2007). Mesoscale flux contributions ranging between 10% and 30% of the turbulent fluxes were a common phenomenon for this transect. There was only one flight with very small mesoscale transport, on a warm sunny day with an air temperature of 26ºC at the Twin Otter flight level and infrared surface temperatures as high as 50ºC. It was the flight with the largest surface temperature difference between water surface of Candle Lake (7.9ºC) and the land around it (27.1ºC). Wind speeds were relatively high, 7.9 m s^{-1} on average.

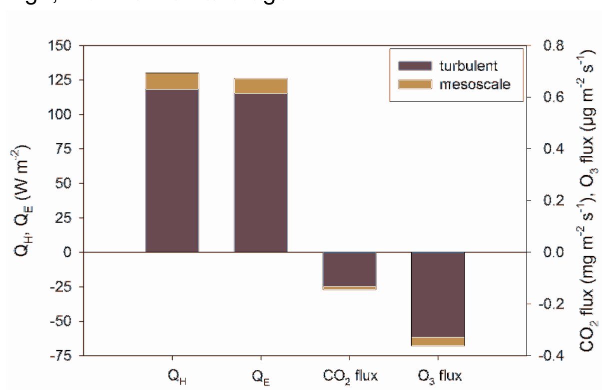

Figure 3: Flux contributions from different scale classes for the entire flight track. Flight BOREAS, 25 May 1994, 1041 – 1116 CST (Mauder et al., 2007, modified).

The largest mesoscale contributions were found for the flight with the smallest surface temperature difference between Candle Lake and the land (2ºC). Wind speeds were moderately high with an average of 4.8 m s^{-1}. The largest mesoscale flux contributions occurred around noon; also in the later afternoon mesoscale flux contributions were high. However in the mornings, mesoscale fluxes were relatively small, usually not much larger than 15% of the turbulent flux, indicating that mesoscale transport mainly occurs in a fully developed convective boundary layer. The mesoscale flux contributions obtained from the wavelet analysis of aircraft data are on the same order as the usual energy balance residuals obtained from simultaneously conducted tower measurements in the same area (Baldocchi and Vogel, 1997; Pattey et al., 1997).

3. A 2-DIMENSIONAL APPROACH TO ESTIMATE MESOSCALE FLUX CONTRIBUTIONS FROM A MULTIPLE TOWER MEASUREMENT SYSTEM

Our goal was to design an experimental set-up that is capable of measuring the turbulent flux without the common underestimation, i.e. a set-up that does not neglect flux contributions that cannot be captured using temporal averaging over 30 min or 60 min. Extending the averaging time to several hours, would be one option (Sakai et al., 2001; Finnigan et al., 2003; Mauder and Foken, 2006). However, such long averaging times are not suitable for many process studies. In addition, if transporting structures are completely stationary, they can never be captured by a single-point measurement regardless of the averaging time.

Such an experimental set-up should be able to provide continuous long-term datasets for turbulent fluxes, as opposed to aircraft measurements, without neglecting low-frequency flux contributions. We focused on the sensible heat flux for a first test, which will show if the measurement approach based on spatial averaging can give larger flux estimates than the conventional temporal eddy-covariance approach. The sensible heat flux $Q_{H,s}$ was computed using a time-spatial average as reference level, which is subtracted from the instantaneous fluctuations, assuming the time-space-averaged vertical wind speed $[w] = 0$.

$$Q_{H,s} = \frac{1}{N} \sum_{t=0}^{30\,\text{min}} \left(w - [w]\right)\left(T - [T]\right). \tag{2}$$

A horizontal observation network consisting of 25 temperature sensors was deployed for measuring the time-space-averaged temperature $[T]$. Careful inter-calibration of sonic anemometer/thermometer and the slow-response temperature sensor network is required for a successful realization of this approach. In contrast, the conventional method for tower-based flux measurements uses the temporal average as reference level.

$$Q_{H,t} = \frac{1}{N} \sum_{t=0}^{30\,\text{min}} \left(w - \overline{w}\right)\left(T - \overline{T}\right). \tag{3}$$

An overview of the experimental set-up is given in Figure 4. An agricultural area in southwest Ottawa, Ontario, Canada served as test site for this experiment (45°18'12" N, 75°46'13" W, 88 m a.s.l.). The area was approximately 3.5 km x 3.5 km. It was surrounded mostly by residential area. The observation period was from 17 May 2007 to 20 June 2007. The main crops were corn, soybean, forage and wheat (4). A small fraction of the observation area in the southwest and in the north was fallow land partially covered by shrubs and low trees. An observation height of 2.60 m above ground level was chosen.

The main site in the center of the observation area was equipped with a Campbell Scientific CSAT3 sonic anemometer/thermometer for measuring w and T. A a Kipp&Zonen CMA6 albedometer and a high-precision temperature sensor of type MetOne 063 in a fan-aspirated radiation shield of type MetOne 076B were deployed to determine the radiation correction for the 25 naturally ventilated HOBO temperature sensors, which is described in Mauder et al. (2008a).

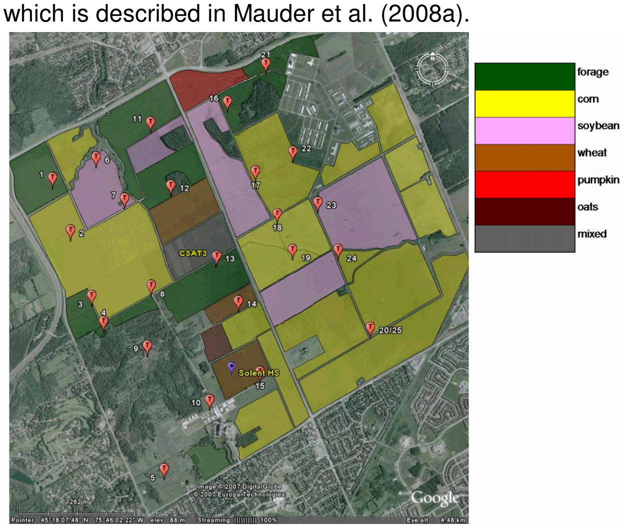

Figure 4: Overview of the observation area. The locations of the 25 HOBO temperature sensors are indicated by red pins labelled with a 'T' and the site number. Coloured polygons indicate the different crop types. Areas not overlaid by a polygon are not cultivated for agriculture (Mauder et al., 2008b).

On 22 May and 23 May 2007, the spatially and the temporally averaged sensible heat flux estimates were almost identical (Figure 5). The weather was overcast or rainy during this period. Temperature maxima ranged between 10°C and 26°C (Figure 6). The following days 24 May and 25 May were much warmer and sunnier; temperature maxima reached more than 30°C. These were also the first two days when larger differences between $Q_{H,s}$ and the conventional temporally averaged heat flux $Q_{H,t}$ were observed. In spite of nearly clear sky conditions and strong solar forcing, $Q_{H,t}$ was lower than

35 W m^{-2}, whereas $Q_{H,s}$ was more than 90 W m^{-2} on 24 May and more than 165 W m^{-2} on 25 May. The maximum difference between $Q_{H,s}$ and $Q_{H,t}$ occurred between 1500 and 1530 Eastern Standard Time (EST) on 25 May, when $Q_{H,t}$ was –84 W m^{-2} and $Q_{H,s}$ was 98 W m^{-2}. Wind speeds were moderately high on these two days ranging between 2.5 and 5.8 m s^{-1}. Wind directions were relatively stable during daytime around west (Mauder et al., 2008b).

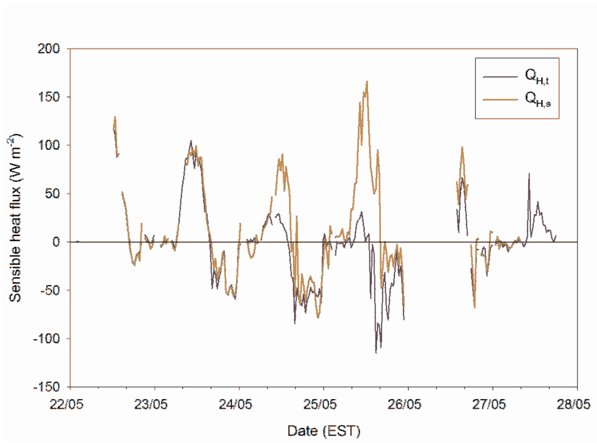

Figure 5: Sensible heat flux estimates from time-spatial ($Q_{H,s}$), and temporal averaging ($Q_{H,t}$). The averaging time is 30 min.

Over the entire 34 day observation period, differences between $Q_{H,t}$ and $Q_{H,t}$ larger than 50 W m^{-2} were found for eight days. For four more days, sensible heat flux estimates from the spatial method were larger by more than 25 W m^{-2} (Mauder et al., 2008b). On these days, differences were typically small in the morning and reached a maximum in the afternoon. On 11 out of 12 of these days, the mean temperature at the central site T was cooler than the time-space averaged temperature [T], sometimes by more than 2°C. At the same time, mean vertical wind velocities w were clearly negative, reaching half hour means of up to –0.15 m s^{-1} (Figure 6).

In summary, the temporally averaged sensible heat flux underestimates the total vertical heat flux, which is computed based on time-space averaging, if cool air is subsiding, T < [T] and w < 0, or if when warm air is rising, T > [T] and w > 0 (Figure 7). The opposite cases, rise of cool air or subsidence of warm air, are highly unlikely due to buoyancy laws, unless there is moist convection involved. No additional flux from the spatially averaging method was observed if only one of these conditions was fulfilled, i.e. only w < 0 and T ≈ [T], or only T < [T] and w ≈ 0 (Figure 5, Figure 6).

The reason why the temporal method underestimates the total vertical flux is because it neglects vertical mass transfer. The mean vertical wind velocity is usually forced to be equal to zero by a coordinate rotation. However, even if the rotation formally eliminates the mean vertical velocity, it cannot account for the mass flow that occurs if the actual vertical wind velocity is not equal to zero.

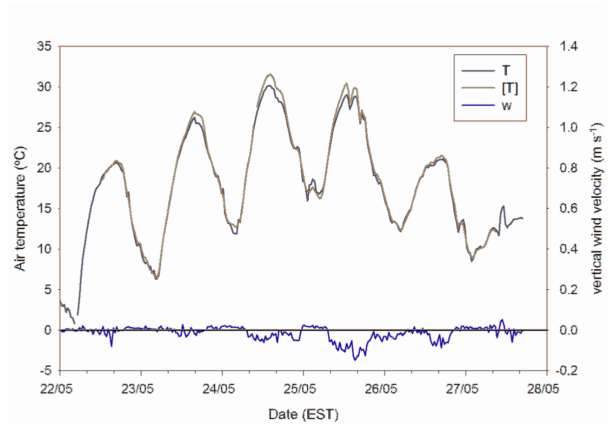

Figure 6: Mean half hourly air temperature averaged over all 25 HOBO sensors [T] and measured at the central site T, plus vertical wind velocity w measured at the central site.

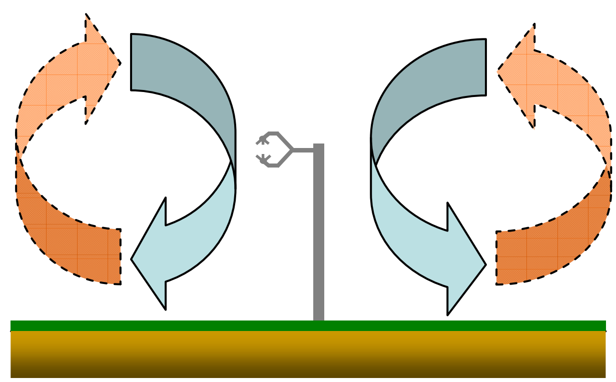

Figure 7: This schematic shows how quasi-stationary circulations cause an underestimation of the total sensible heat flux when using the temporal EC method. Blue arrows indicate subsidence of cool air, and orange arrows indicate rise of warm air. The single-point sonic measurement in the centre of the schematic is not able to resolve quasi-stationary eddies. This is only possible by spatial averaging.

4. CONCLUSIONS

Mesoscale flux contributions between 10% – 30% were found from aircraft measurements. This is on the order of the energy balance residuals that were measured at single-tower sites near the flight track. We found experimental evidence for the missing flux contributions that cause energy balance closure problems. The percentage of mesoscale flux contributions was different for each scalar and also for each flight. Energy balance correction for the sensible and the latent heat flux according to the Bowen ratio cannot be justified. Correcting CO_2 fluxes according to the energy balance residual could also lead to unrealistic results. New approaches based on information about the spatial data are needed to obtain more realistic flux estimates.

Large-scale organized structures or quasi-stationary circulations account for a significant amount of transport between the earth's surface and the atmosphere, even in the lower surface layer. Fluxes are underestimated when using the temporal eddy-covariance method, since these circulations are not captured. The flux contribution of these circulations was experimentally quantified through time-spatial averaging of 1-dimensional aircraft measurements with a flight track of 115 km length at a height of 30 m and a 2-dimensional spatial temperature sensor network over an area of 3.5 km x 3.5 km at a height of 2.6 m. For future studies, an extension of the spatial network to measure different scalars like water vapor and carbon dioxide would be desirable.

5. ACKNOWLEDGEMENTS

We are grateful to Doug Glowenlock, manager of the Canadian Food Inspection Agency research farm in Ottawa, Bert Moore, manager of the Greenbelt research farm in Ottawa, for their cooperation during the realisation of the experiment.

6. REFERENCES

Aubinet, M., A. Grelle, A. Ibrom, Ü. Rannik, J. Moncrieff, T. Foken, A. S. Kowalski, P. H. Martin, P. Berbigier, C. Bernhofer, R. Clement, J. Elbers, A. Granier, T. Grünwald, K. Morgenstern, K. Pilegaard, C. Rebmann, W. Snijders, R. Valentini, and T. Vesala, 2000: Estimates of the annual net carbon and water exchange of forests: The EUROFLUX methodology. *Adv. Ecol. Res.*, **30,** 113-175.

Baldocchi, D. D. and C. A. Vogel, 1997: Seasonal variation of energy and water vapor exchange rates above and below a boreal jack pine forest canopy. *J. Geophys. Res.*, **102,** 28939-28951.

Chahuneau, F., R. L. Desjardins, E. Brach, and R. Verdon, 1989: A micrometeorological facility for eddy flux measurements of CO_2 and H_2O. *J. Atmos. Oceanic Technol.*, **6,** 193-200.

Desjardins, R. L., 1985: Carbon dioxide budget of maize. *Agric. For. Meteor.*, **36,** 29-41.

Finnigan, J. J., R. Clement, Y. Malhi, R. Leuning, and H. A. Cleugh, 2003: A re-evaluation of long-term flux measurement techniques, Part I: Averaging and coordinate rotation. *Bound.-Layer Meteor.*, **107,** 1-48.

Hall, F. G., D. E. Knapp, and K. F. Huemmerich, 1997: Physically based classification and satellite mapping of biophysical characteristics in the southern boreal forest. *J. Geophys. Res.*, **102,** 29567-2958.

MacPherson, J. I., 1996: NRC Twin Otter operations in BOREAS 1994. Report LTR-FR-129, 32 pp.

MacPherson, J. I., D. L. Marcotte, and J. E. Jordan, 2001: The NRC Atmospheric Research Aircraft. *Journal of the Canadian Aeronautics and Space Institute*, **47,** 147-157.

Mauder, M. and T. Foken, 2006: Impact of post-field data processing on eddy covariance flux estimates and energy balance closure. *Meteor. Z.*, **15,** 597-609.

Mauder, M., R. L. Desjardins, and J. I. MacPherson, 2007: Scale analysis of airborne flux measurements over heterogeneous terrain in a boreal ecosystem. *J. Geophys. Res.*, **112,** D13112, doi: 10.1029/2006JD008133.

Mauder, M., R. L. Desjardins, Z. Gao, and R. van Haarlem, 2008a: Errors of naturally ventilated air temperature measurements in a spatial observation network. *J. Atmos. Oceanic Technol.***,** subm.

Mauder, M., R. L. Desjardins, E. Pattey, Z. Gao, and R. van Haarlem, 2008b: Measurement of the sensible eddy heat flux based on spatial averaging of continuous ground-based observations. *Bound.-Layer Meteor.***,** subm.

Pattey, E., R. L. Desjardins, and G. St-Amour, 1997: Mass and energy exchanges over a black spruce forest during key periods of BOREAS 1994. *J. Geophys. Res.*, **102,** 28967-2875.

Sakai, R. K., D. R. Fitzjarrald, and K. E. Moore, 2001: Importance of low-frequency contributions to eddy fluxes observed over rough surfaces. *J. Appl. Meteor.*, **40,** 2178-2192.

Wilson, K., A. Goldstein, E. Falge, M. Aubinet, D. Baldocchi, P. Berbigier, C. Bernhofer, R. Ceulemans, H. Dolman, and C. Field, 2002: Energy balance closure at FLUXNET sites. *Agric. For. Meteor.*, **113,** 223-243.